



## A Novel Control Strategy of an Islanded Microgrid Based on Virtual Flux Droop Control and Direct Flux Fuzzy Control

S. Khanabdal<sup>a</sup>, M. Banejad<sup>a</sup>, F. Blaabjerg<sup>b</sup>, N. Hosseinzadeh<sup>c</sup>

<sup>a</sup> Department of Electrical Engineering, Shahrood University of Technology, Shahrood, Iran

<sup>b</sup> Department of Energy Technology, Aalborg University, Aalborg, Denmark

<sup>c</sup> School of Engineering, Deakin University, Geelong, Australia

### PAPER INFO

#### Paper history:

Received 21 December 2020

Received in revised form 12 March 2021

Accepted 13 March 2021

#### Keywords:

Islanded Microgrid

Virtual Flux Droop Control

Fuzzy Logic Control

Optimal Duty Cycle

### ABSTRACT

This paper proposes a novel control strategy of an islanded microgrid based on virtual flux droop (VFD) control. In the conventional VFD method, the direct flux control (DFC) technique is used to generate the switching signals using the hysteresis regulators and a switching look-up table. Therefore, the voltage and the current ripples are inevitable. Moreover, as a single switching vector is applied in each control period and none of the switching vectors can produce the desired voltage, the desired dynamic performance is not achieved. Here, a novel direct flux fuzzy control (DFFC) technique is proposed to choose the best switching vector based on fuzzy logic. Furthermore, only a fraction of the control period is allocated to an appropriate active switching vector which is selected by the DFFC technique whereas the rest of the time is allocated to a null vector. The duty cycle of the selected active switching vector is optimized using a simple and robust mechanism. In order to evaluate the performance of the proposed method, an islanded microgrid and the proposed control strategy is simulated in Matlab/Simulink software. The results prove that the dynamic performance response is improved and the demanded load power is proportionately shared between the sources, while the voltage and current ripples are significantly reduced.

doi: 10.5829/ije.2021.34.05b.21

## 1. INTRODUCTION

In recent decades, distributed generation (DG) has attracted growing attention of researchers as an efficient solution for worldwide demand to reduce the reliance on fossil fuels and increase the use of renewable energy. In this regard, the concept of microgrid plays an important role in moving towards the realization of the future smart grids by integrating multiple DG units using renewable energy resources, energy storage systems and local loads with a coordinated control strategy. Inverters are usually employed to interface DG units to the microgrid. As a result, they should be connected in parallel through the point of common coupling (PCC) which increases the reliability of the system by providing redundancy [1-6].

Microgrid is able to operate in grid connected or islanded mode. However, the control of an islanded

microgrid is a more challenging issue because of no access to the main grid. In this case, maintaining the stable regulation of the voltage and frequency is important as well as proportional sharing the load among multiple parallel inverters in order to achieve better power management and to avoid overloading of some inverters [7-11]. Therefore, an appropriate control strategy should be applied to meet the requirement.

Droop control strategy is widely used in the islanded microgrid which emulates the behavior of synchronous generators without the dependency on communication. Therefore, the “plug and play” feature is achieved, with the result that the expansion of such a system becomes easier which allows to replace or add one unit with no need to stop the whole system. Based on this strategy, the frequency is adjusted as a function of active power and the voltage amplitude of the inverter is regulated as a

\*Corresponding Author Institutional Email:  
[m.banejad@shahroodut.ac.ir](mailto:m.banejad@shahroodut.ac.ir) (M. Banejad)

function of reactive power. Despite the advantages of the droop control strategy, it suffers from drawbacks that the unavoidable deviations of frequency and voltage amplitude in the steady state condition, poor dynamic stability of active power sharing controller and poor reactive power sharing [12-14].

Several improved control methods were proposed in the literature to solve the above problems. One group of them try to revise the overall control strategy through optimization and implementation of modern control theory. A novel secondary control scheme was proposed by Lou et al. [15] for voltage and frequency restoration. It uses the distributed model predictive control for voltage regulation. Moreover, a distributed finite time observer is employed to realize the frequency adjustment and proper active power sharing and frequency restoration. The effectiveness of the droop control strategy in accurate power sharing was improved by Lai et al. [16] which is based on the distributed cooperative control scheme. It introduces a pinning-based frequency/voltage controller using a distributed voltage observer and employed a consensus power controller to generate nominal values for droop control of DGs. A distributed secondary control based on droop control strategy was proposed by Wu and Shen [17] for stability enhancement of microgrid which uses supplementary control variables. Small signal modeling of the system is employed to define an optimization problem and consequently tune the control parameters robustly. An optimized droop control based on a dynamic model of the microgrid is proposed by Yu et al. [18]. Firstly, a precise small signal model of the whole microgrid and the droop controller is derived. Consequently, the dynamic stability of the system is investigated by the eigenvalue analysis method. Then, a genetic algorithm is employed to find the optimal values of key parameters. In the case of optimization, the optimum values should be found after each change of the parameters of the system. However, the mentioned control strategies are usually complicated and complex coordinated transformations are also needed. Moreover, they required mostly high speed communication to achieve precise power sharing.

Another group of methods in the literature proposes to add compensatory terms to the droop equations to enhance the performance of the conventional droop control. In order to enhance the power loop dynamics, a mode-adaptive droop control method was proposed by Kim et al. [19], where the derivative controller is added in the relationship of the frequency-active power and the integral controller is added in the relationship of the voltage amplitude-reactive power. An improved proportional power sharing strategy was proposed by Zhang et al. [20] which can deal with the problem of the coupling between the active and reactive power in the droop control strategy. In this regard, integral controllers are employed to generate the compensatory terms in the

proposed droop equations. An improved droop controller is proposed by Zhong [21] which added the load voltage drop with an amplifier to the droop characteristics. As a result, the proposed control strategy is robust to computational errors, disturbances, noises and parameter drifts. However, in this group of methods, complex transformations are needed and communication with the central control unit of the microgrid is needed to send measured parameters and receive reference values which are required to generate compensatory terms. Therefore, the reliability of the control strategy is degraded.

The proper power sharing in an islanded microgrid can be achieved by changing the parameters and equations of the droop method. The output voltage phase is employed instead of frequency reported in literature [22] to improve the power sharing accuracy and to effectively reduce the circulating current. Chen et al. [23] proposed  $P-\dot{V}$  droop control; where  $\dot{V}$  represents the time rate of change of the output voltage reference. As a result, the effect of mismatched line impedance is mitigated and the accuracy of the active power sharing is improved. In order to improve the reactive power sharing accuracy, a  $Q-\dot{V}$  droop control method was proposed by Lee et al. [24]. But the effectiveness of this method is degraded by the output voltage variation and a restoration technique is required to avoid it. To deal with this problem, a modified  $Q-\dot{V}$  was proposed by Zhou and Cheng [25], where a novel  $\dot{V}$  restoration mechanism is employed to pull the  $\dot{V}$  back to zero. However, these strategies use one of the equations of conventional droop control which leads to a decrease in the power sharing accuracy. In this regard, a new control strategy called virtual flux droop was proposed by Hu et al. [26], where the phase angle difference and the virtual flux amplitude are respectively being used instead of the frequency and the voltage amplitude of the inverter. Therefore, a simple control strategy is achieved while there is no need to complex coordinate transformation as well as PI controllers are avoided. In the structure of the VFD control method, direct flux control is employed to generate the switching signals, which works similarly to direct torque control and direct power control. Therefore, simple structure, fast dynamic response and robustness against parameter variation are the advantages. However, DFC suffers from some disadvantages which are mainly due to using the hysteresis regulators. As a result, the ripples appear in the virtual flux amplitude and the phase angle difference which can be reflected on the voltage and the current waveforms and affect power quality.

This paper proposes a novel microgrid control strategy by using fuzzy logic control to overcome the disadvantages of the conventional virtual flux droop control. Fuzzy logic control is considered as an effective approach in case of complicated processes, where the mathematical model does not exist or it is nonlinear.

Regarding that the VFD control is a nonlinear method, it is combined with direct flux fuzzy control as proposed in this paper. In the structure of DFFC, a fuzzy switching table is employed to replace the conventional switching look-up table and hysteresis regulators. Moreover, instead of applying a single switching vector throughout each control period, only a fraction of the control period is allocated to the active switching vector which is selected by DFFC whereas a null vector is applied for the rest of the time. Furthermore, a simple and robust method is proposed to compute the optimal duty ratio of the active switching vector. As a result, the performance of the microgrid control strategy in power sharing is improved by reducing the voltage and the current ripples. Therefore, the main contributions of this paper are:

1. Developing the virtual flux droop control based on direct flux fuzzy control

2. Applying duty cycle control to the microgrid control strategy by the proposed duty ratio optimization method.

The rest of this paper is organized as follows: Section 2 describes mathematically the VFD control. The microgrid control strategy is discussed in section 3, so that, firstly the conventional method is briefly described. Then, the proposed control strategy is explained in detail. In order to validate the effectiveness of the proposed strategy for controlling the islanded microgrid, the simulation is carried out in the environment of Matlab/Simulink and the results are reported and also compared with the conventional method in section 4. Finally, this paper is summarized in section 5.

## 2. PRINCIPLE OF VIRTUAL FLUX DROOP METHOD

In an islanded microgrid with parallel configuration, the inverters are connected to the point of common coupling (PCC) through the line impedances as shown in Figure 1. The mathematical equation of this equivalent circuit can be written using Kirchhoff's voltage law stated as follows:

$$V_i = R_i I_i + L_i \frac{dI_i}{dt} + E \quad (1)$$

where  $E$  and  $V_i$  are the voltages of the PCC and the inverter, respectively. Moreover,  $I_i$  is the line current.

In addition,  $R_i$  and  $L_i$  are the line resistance and inductance, respectively. Furthermore, the number of the inverter is denoted by the subscript "i".

The supplied power by the inverter to the PCC is calculated as follows:

$$S_i = P_i + jQ_i = E \times I_i^* \quad (2)$$

where  $S_i$  is complex power,  $P_i$  is active power and  $Q_i$  is reactive power. The superscript "\*" denotes the complex conjugate.

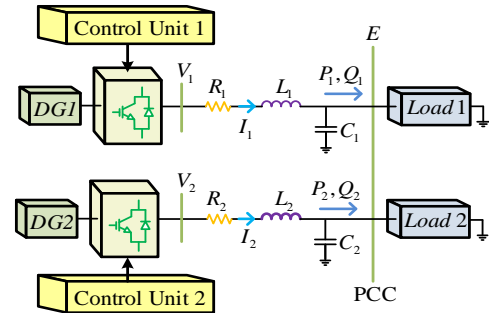


Figure 1. An islanded microgrid with parallel inverters

Similar to electrical machines, in which the flux is defined as time integral of voltage, the virtual flux vectors are defined [26]:

$$\psi_i = \int V_i dt = \frac{|V_i|}{\omega} e^{j\varphi_i} \quad (3)$$

$$\psi_E = \int E dt = \frac{|E|}{\omega} e^{j\varphi_E} \quad (4)$$

In these equations,  $\psi_i$  and  $\psi_E$  are the virtual flux vectors of the inverter and the PCC, respectively,  $\varphi_i$  and  $\varphi_E$  are their angles, and  $\omega$  is the angular frequency.

It is assumed for simplicity that the line is highly inductive and the line resistance is negligible. As a result, the line current can be written in terms of virtual fluxes as:

$$I_i = \frac{1}{L_i} (\psi_i - \psi_E) \quad (5)$$

Substituting the line current from Equation (5) and the voltage of the PCC in terms of virtual flux from Equation (4) in Equation (2) and then separating its real and imaginary parts, the active power and the reactive power are obtained as follows:

$$P_i = \frac{\omega}{L_i} |\psi_i| |\psi_E| \sin(\delta_i) \quad (6)$$

$$Q_i = \frac{\omega}{L_i} (|\psi_i| |\psi_E| \cos(\delta_i) - |\psi_E|^2) \quad (7)$$

where  $\delta_i = \varphi_i - \varphi_E$ . Since  $\delta_i$  is also equal to the phase angle difference between the voltages of the PCC and the inverter, which is typically small, it can be considered that,  $\sin \delta \cong \delta$  and  $\cos \delta \cong 1$  [24, 26-28] which result in:

$$P_i = \frac{\omega}{L_i} |\psi_i| |\psi_E| \delta_i \quad (8)$$

$$Q_i = \frac{\omega}{L_i} |\psi_E| (|\psi_i| - |\psi_E|) \quad (9)$$

The above equations imply that the active power and the reactive power are respectively coupled with the phase angle difference and amplitude difference between the virtual fluxes of the inverter and the PCC. Thus, the mathematical equations of virtual flux droop control for the inverter are achieved [26]:

$$\delta_i^{com} = \delta_i^n - k_{\delta_i} (P_i^n - P_i) \quad (10)$$

$$|\psi_i^{com}| = |\psi_i^n| - k_{\psi_i} (Q_i^n - Q_i) \quad (11)$$

where  $P_i^n$  and  $Q_i^n$  are nominal active power and nominal reactive power, respectively,  $\delta_i^n$  is nominal phase angle difference,  $|\psi_i^n|$  is the nominal virtual flux amplitude of the inverter,  $k_{\delta_i}$  and  $k_{\psi_i}$  are the slopes of the droop characteristics. Moreover,  $\delta_i^{com}$  and  $|\psi_i^{com}|$  are respectively the command values of the phase angle difference and the virtual flux amplitude of the inverter.

### 3. MICROGRID CONTROL STRATEGY

#### 3. 1. The Conventional Method Based on DFC

The conventional control strategy of the islanded microgrid based on the virtual flux droop control and direct flux control is shown in Figure 2. Firstly, the command values of the phase angle difference between the virtual fluxes of the inverter and the PCC and the virtual flux amplitude of the inverter are specified by the VFD control method. Then, DFC is employed to apply them to the inverters. In this regard, the output voltage of the inverter is calculated using the current state of the inverter switches. Subsequently, the virtual flux vector of the inverter is estimated using Equation (3). The amplitude of the estimated virtual flux of the inverter is subtracted from its command value which is obtained from VFD and therefore the error of the virtual flux amplitude is generated in this way. On the other side, the angle of the virtual flux vector of the PCC is obtained using a virtual set of three-phase AC voltage with the nominal frequency of the grid. Then, the phase angle difference between the virtual fluxes of the inverter and the PCC can be estimated by subtracting the angle of the estimated virtual flux vector of the inverter from the angle of the virtual flux vector of the PCC. Subsequently, the estimated phase angle difference is subtracted from its command value obtained from VFD, and consequently, the error of the phase angle difference is computed. On the other hand, the  $\alpha - \beta$  plane is divided into six sections and the section, where the virtual flux vector of the inverter is located, is determined.

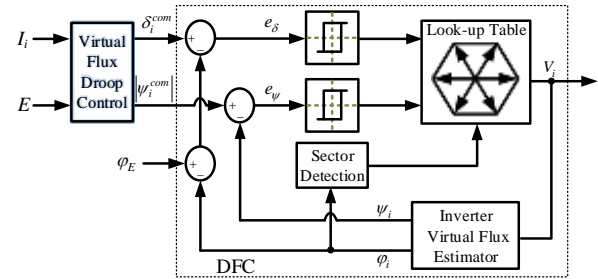


**Figure 2.** The conventional microgrid control strategy based on VFD control and DFC

In the DFC scheme, the errors of the virtual flux amplitude and the phase angle difference are entered into the hysteresis regulators. Eventually, the appropriate switching vector to apply to the inverter is selected from a look-up table, which has three inputs, including the number of the section, where the virtual flux vector of the inverter is located, along with the outputs of the hysteresis regulators. In this method, regardless of where the virtual flux vector of the inverter is located, the choice of the best switching vector is independent of the amplitude of the flux and angle errors and depends only on the sign of the phase angle difference and the virtual flux amplitude errors specified by the hysteresis regulators. As the hysteresis band increases, the switching frequency decreases; nevertheless, the accuracy of voltage and frequency control is reduced. As the hysteresis band decreases, although the accuracy of voltage and frequency control increases, the switching frequency increases. The use of the hysteresis regulators in the structure of the DFC leads to ripples of the virtual flux vector of the inverter and the phase angle difference; therefore, may be reflected on current and voltage THD indices.

**3. 2. The Proposed Method Based on Dffc** This paper aims to deal with the disadvantages of the conventional microgrid control strategy caused by the direct flux control. Figure 3 shows the proposed microgrid control strategy which consists of VFD control, DFFC and duty ratio optimization. The following describes each part.

**1) Virtual Flux Droop Control:** As described in section 2, the proportional power sharing between the DGs is achieved by the VFD control method. For this reason, the values of the active power and the reactive power injected into the PCC are calculated and the command values for the phase angle difference and the virtual flux amplitude of the inverter are obtained by Equations (10) and (11).

**2) Direct Flux Fuzzy Control:** Fuzzy logic makes it possible to control systems without knowing the mathematical model of the process [29-31]. As a result, a

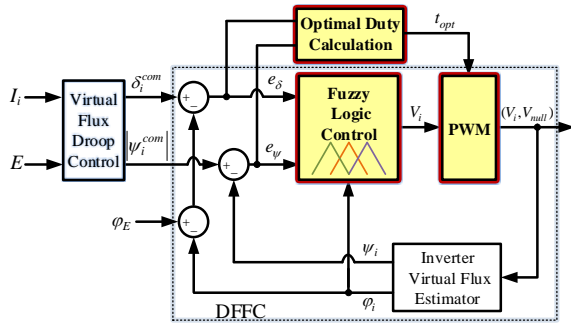


**Figure 3.** The proposed microgrid control strategy based on VFD control, DFFC and duty ratio optimization

novel control scheme to select the appropriate switching vector is proposed in this paper. First, the switching vector and subsequently, the three-phase inverter output voltages are calculated using the current state of the inverter switches as reported in literature [32]:

$$\begin{bmatrix} v_a \\ v_b \\ v_c \end{bmatrix} = V_{dc} \cdot \begin{bmatrix} \frac{2}{3} & \frac{-1}{3} & \frac{-1}{3} \\ \frac{-1}{3} & \frac{2}{3} & \frac{-1}{3} \\ \frac{-1}{3} & \frac{-1}{3} & \frac{2}{3} \end{bmatrix} \times \begin{bmatrix} s_a \\ s_b \\ s_c \end{bmatrix} \quad (12)$$

$$\begin{bmatrix} V_\alpha \\ V_\beta \end{bmatrix} = \begin{bmatrix} \frac{2}{3} & \frac{-1}{3} & \frac{-1}{3} \\ 0 & \frac{\sqrt{3}}{3} & \frac{-\sqrt{3}}{3} \end{bmatrix} \times \begin{bmatrix} v_a \\ v_b \\ v_c \end{bmatrix} \quad (13)$$

$$V_i = V_\alpha + jV_\beta \quad (14)$$

where  $V_{dc}$  is the input voltage of the inverter,  $v_a, v_b$  and  $v_c$  are the three-phase inverter output voltages,  $s_a, s_b$  and  $s_c$  are the current state of the inverter switches.  $s_i = 0$  ( $i = a, b, c$ ), while the related switch is open and  $s_i = 1$  ( $i = a, b, c$ ), while the related switch is closed. In addition,  $V_\alpha$  and  $V_\beta$  are the component of the inverter voltage in the  $\alpha - \beta$  plane.

The phase angle and the virtual flux amplitude of the inverter are estimated using Equation (3). On the other hand, the phase angle of the virtual flux vector of the PCC is calculated using a set of three-phase AC voltage with the nominal frequency. As a result, the estimated phase angle difference between the virtual fluxes of the inverter and the PCC can be obtained. Finally, the estimated values of the phase angle difference and the virtual flux amplitude of the inverter are compared with their commands.

In DFFC, the fuzzy logic controller (FLC) is replaced with the hysteresis regulators and the switching look-up table which are used in DFC. The inputs of FLC are the phase angle difference and the virtual flux amplitude of the inverter errors as well as the phase angle of the current

virtual flux of the inverter. Consequently, the output of FLC is the best switching vector that should be applied to the inverter. As shown in Figure 4, an FLC is generally composed of four principal parts, namely Fuzzification, Fuzzy rule base, Inference system and Defuzzification. In the process of Fuzzification, the numerical input variables are converted to fuzzy values using membership functions (MFs) shown in Figures 5 to 7, where the triangular MFs are utilized. The error of the phase angle difference, i.e.  $e_\delta$ , can be negative large (NL), negative small (NS), zero (Z), positive small (PS) and positive large (PL). Moreover, the error of the virtual flux amplitude i.e.  $e_\psi$  can be negative (N), zero (Z), and positive (P). In addition, the phase angle of the virtual flux of the inverter in the  $\alpha - \beta$  plane, i.e.  $\theta$ , can change in the range of  $[0 - 2\pi]$  which is divided into six sections and the corresponding MFs are denoted as  $\theta_1$  to  $\theta_6$ . The number of switching vectors equals  $2^3=8$  including six active vectors and two zero vectors as shown in Figure 8. As a result, seven singleton subsets including one null vector and six active vectors are assigned to the MFs of the output variable, which are denoted by  $V_0$  to  $V_6$ , as shown in Figure 9. The FLC specifies the relationship between the inputs and the output using fuzzy rule base, as shown in Table 1. Then, the appropriate control rules at each time are evaluated by the fuzzy inference mechanism which is Mamdani's procedure based on a min-max decision in this paper. If the MF values of the input variables, i.e.  $e_\delta$ ,  $e_\psi$  and  $\theta$  are respectively  $\mu_\phi$ ,  $\mu_\psi$ ,  $\mu_\theta$  and the MF value of the output variable is  $\mu_V$ , the corresponding weighting factor  $a_i$  for  $i^{th}$  rule is achieved as follows:

$$a_i = \min(\mu_{\phi_i}, \mu_{\psi_i}, \mu_{\theta_i}) \quad (15)$$

$$\mu'_{V_i} = \max(a_i, \mu_{V_i}) \quad (16)$$

Finally, the fuzzy values are converted back into crisp values which is the best switching vector between  $V_0$  to  $V_6$  in Defuzzification process using the SOP method:

$$\mu'_{V_{out}} = \max_{i=1}^{90}(\mu'_{V_i}) \quad (17)$$

**3) Duty Ratio Optimization:** As the desired voltage which is needed to provide the appropriate changes in the

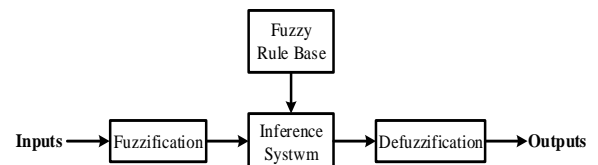


**Figure 4.** Block diagram of FLC

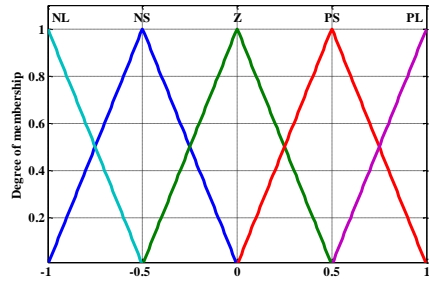


Figure 5. Membership functions of  $e_\delta$

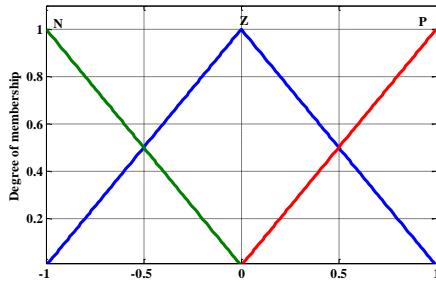


Figure 6. Membership functions of  $e_\psi$

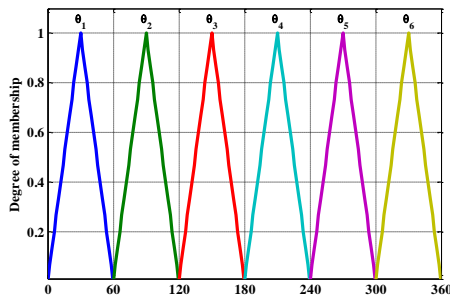


Figure 7. Membership functions of  $\theta$

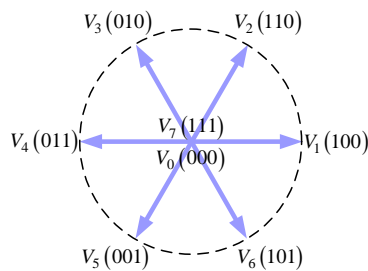


Figure 8. Switching vectors in the  $\alpha - \beta$  plane

TABLE 1. Switching Vector Table based on FLC

$e_\psi$	$e_\delta$	$\theta_1$	$\theta_2$	$\theta_3$	$\theta_4$	$\theta_5$
	NL	$V_5$	$V_6$	$V_1$	$V_2$	$V_3$
	NS	$V_5$	$V_6$	$V_1$	$V_2$	$V_3$
N	Z	$V_0$	$V_0$	$V_0$	$V_0$	$V_0$

	PS	$V_3$	$V_4$	$V_5$	$V_6$	$V_1$	$V_2$
	PL	$V_3$	$V_4$	$V_5$	$V_6$	$V_1$	$V_2$
	NL	$V_6$	$V_1$	$V_2$	$V_3$	$V_4$	$V_5$
	NS	$V_6$	$V_1$	$V_2$	$V_3$	$V_4$	$V_5$
Z	Z	$V_0$	$V_0$	$V_0$	$V_0$	$V_0$	$V_0$
	PS	$V_2$	$V_3$	$V_4$	$V_5$	$V_6$	$V_1$
	PL	$V_2$	$V_3$	$V_4$	$V_5$	$V_6$	$V_1$
	NL	$V_6$	$V_1$	$V_2$	$V_3$	$V_4$	$V_5$
	NS	$V_6$	$V_1$	$V_2$	$V_3$	$V_4$	$V_5$
P	Z	$V_0$	$V_0$	$V_0$	$V_0$	$V_0$	$V_0$
	PS	$V_2$	$V_3$	$V_4$	$V_5$	$V_6$	$V_1$
	PL	$V_2$	$V_3$	$V_4$	$V_5$	$V_6$	$V_1$

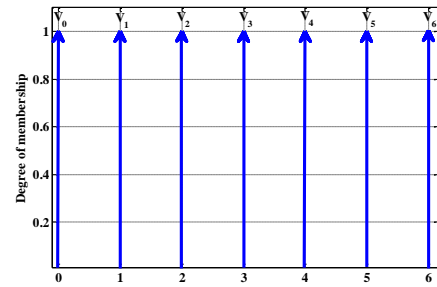


Figure 9. Membership functions of the output

phase angle and amplitude of the inverter virtual flux cannot be generated by any of the switching vectors, the virtual flux ripples is unavoidable. A solution to solve this issue, as proposed in this paper, is to apply two switching vectors during each control period instead of a single switching vector which fails to reduce the voltage and current ripples to the minimum values. This idea has already been used in the induction motor drives based on DTC and MPTC and now generalized in the application of power sharing in the islanding microgrid in this paper. As a result, only a fraction of the control period is allocated for the active vector which is selected from DFFC and a null vector is applied to the inverter during the rest of the time. The optimal duty ratio  $d$  for the active vector is obtained by:

$$d = \left| \frac{e_\delta}{C_\delta} \right| + \left| \frac{e_\psi}{C_\psi} \right| = \left| \frac{\delta^{com} - \delta^{est}(k)}{C_\delta} \right| + \left| \frac{|\psi|^{com} - |\psi|^{est}(k)}{C_\psi} \right| \quad (18)$$

where  $\delta^{est}(k)$  and  $|\psi|^{est}(k)$  are respectively the estimated values for the phase angle difference and the virtual flux amplitude of the inverter at the  $k^{th}$  instant;  $C_\delta$  and  $C_\psi$  are two positive coefficients. As can be seen, the duty ratio is obtained in a simple, fast and robust method without dependency on the grid parameters.

4. SIMULATION RESULTS

In order to study the performance of the proposed method, the islanded microgrid shown in Figure 1 is simulated in the MATLAB/Simulink software environment. The results obtained from applying the proposed control scheme are compared with the conventional method. The simulation parameters of the islanded microgrid are listed in Table 2. A step decrease of the load power occurs at t=1s. Then, the load power is increased to its initial value at t=2s.

Based on the conventional method and the proposed control strategy, Figures 10 and 11 show the PCC voltage and its THD spectra respectively. As can be seen, in spite of the load change, the voltage is maintained within the allowable limit ( $\pm 5\%$ ) using the proposed method, while

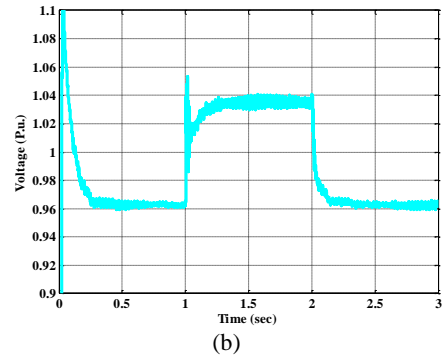


Figure 10. PCC voltage: (a) Conventional method (b) Proposed method

the voltage changes are greater than the allowable value based on the conventional method. Moreover, the voltage ripple using the proposed method is lower than the conventional method, which improves the THD index.

The three-phase injected current of DG1 into the PCC and its THD spectra are respectively shown in Figures 12 and 13. It can be seen that the THD index based on the proposed method is less than the conventional method which leads to less current ripples.

The injected power of DGs to the PCC is shown in Figure 14. The load is modeled as a constant impedance. Therefore, the power which is absorbed by the load, is proportional to the square of the PCC voltage. In both methods, good dynamic performance is observed in response to the load changes. However, due to the better performance of the proposed method in voltage control the voltage amplitude in the conventional method is

TABLE 2. Microgrid and Control Parameters

Item	Value
Line Resistance	0.04 $\Omega$
Line Inductance	6 mH
Tie- line Resistance	1.5 $\Omega$
Tie-line Inductance	12 mH
Filter Capacitance	120 $\mu$ F
Nominal Voltage	3600 V
Nominal Frequency	60 Hz
DGs Output Voltage	10 kV
Nominal Flux Amplitude	7.797 Wb
Nominal Active Power 1	1650 kW
Nominal Reactive Power 1	800 kVar
Nominal Active Power 2	1300 kW
Nominal Reactive Power 2	600 kVar
Slope of P – $\delta$ Droop 1	$-1.67 \times 10^{-8}$ rad/W
Slope of Q – $ V $ Droop 1	$-2.65 \times 10^{-6}$ Wb/Var
Slope of P – $\delta$ Droop 2	$-1.54 \times 10^{-7}$ rad/W
Slope of Q – $ V $ Droop 2	$-2.55 \times 10^{-6}$ Wb/Var

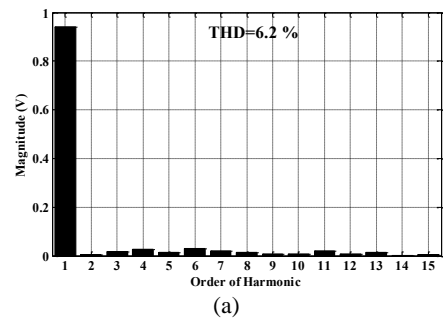
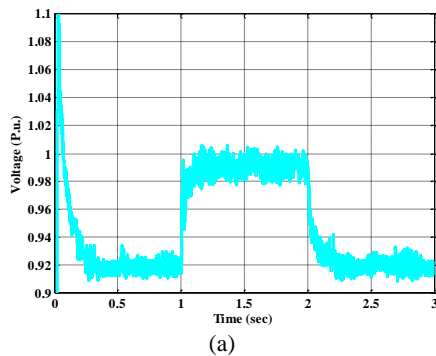
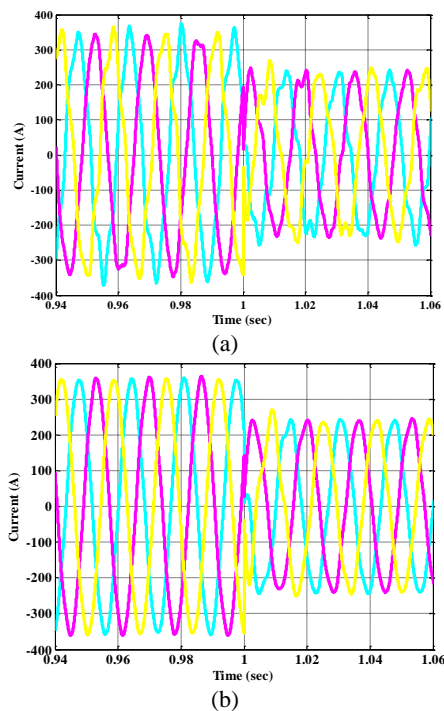
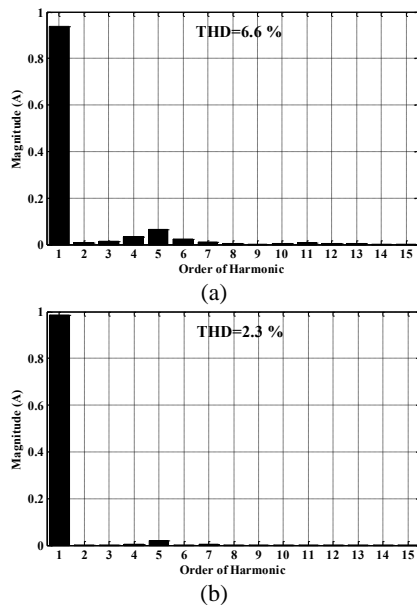


Figure 11. THD spectra of the PCC voltage: (a) Conventional method (b) Proposed method



**Figure 12.** Injected current of DG1 to the PCC: (a) Conventional method (b) Proposed method

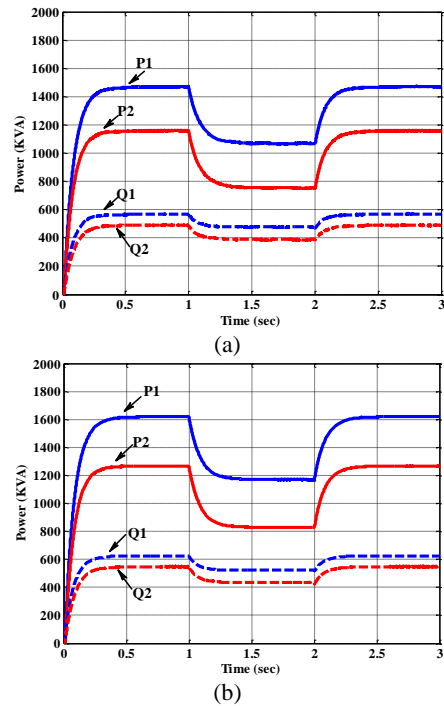


**Figure 13.** THD spectra of injected current of DG1: (a) Conventional method (b) Proposed method

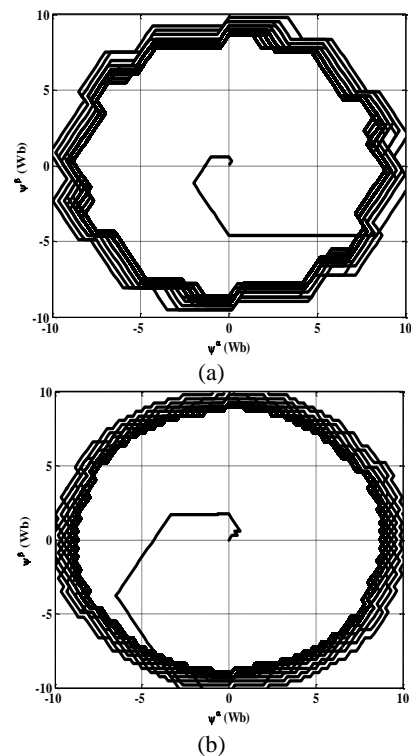
lower than the proposed method, which reduces the power injection in the conventional method.

Figure 15 shows the virtual flux vector trajectory of inverter 1 in the  $\alpha - \beta$  plane. The aim of the virtual flux control of the inverters is to enable them to have the specified amplitude and specific relative distance to the virtual flux vector of the PCC. The tip of the virtual flux

trajectory is closer to the circle using the proposed method, which proves better dynamic performance compared to the conventional method.



**Figure 14.** Injected powers of DGs to the PCC: (a) Conventional method (b) Proposed method



**Figure 15.** Virtual flux trajectory of Inverter 1: (a) Conventional method (b) Proposed method

## 5. CONCLUSION

The use of hysteresis regulators in the DFC method results in the current and voltage ripples. In addition, since none of the switching vectors can generate the desired voltage, the accuracy of the microgrid control strategy decreases and the desired dynamic performance cannot be achieved. In this paper, a novel control strategy of an islanded microgrid was proposed. First, using the virtual flux droop control, the command values i.e. the phase angle difference and the virtual flux amplitude of the inverter, were obtained. Then, the proposed fuzzy based control was employed to select the best switching vector to apply to the inverter. As a result, an effective control method was obtained, while there was no need to use PI controllers or hysteresis regulators. Moreover, the duty cycle of the selected active switching vector was optimally calculated using a simple and robust method whereas the rest of the time of the control period was allocated to the null vector. Therefore, voltage and current ripples were significantly reduced. The proposed method was evaluated using simulation in MATLAB/Simulink software environment and was compared with the conventional method based on the VFD and the DFC. The results showed that the proposed method can proportionally share the power between DGs while the voltage and current ripples were also reduced significantly.

## 6. REFERENCES

- Chen, Y., Guerrero, J. M., Shuai, Z., Chen, Z., Zhou, L., and Luo, A., "Fast reactive power sharing, circulating current and resonance suppression for parallel inverters using resistive-capacitive output impedance," *IEEE Transactions on Power Electronics*, Vol. 31, (2016), 5524-5537. DOI: 10.1109/TPEL.2015.2493103.
- Zhong, Q. -C., and Hornik, T., "Parallel operation of inverters," in Control of Power Inverters in Renewable Energy and Smart Grid Integration, *John Wiley and Sons*, London, (2013), 297-333, (Chapter 19). DOI: 10.1002/9781118481806.ch19.
- Hosseinzadeh, N., Khanabdal, S., Al-Jabri, Y., Al-Abri, R., Hinai, A., and Banejad, M., "Voltage stability of microgrids," in Variability, Scalability and Stability of Microgrids, *IET*, London, (2019), 327-376, (Chapter 10). DOI: 10.1049/PBPO139E\_ch10.
- Sagar, G. V. R., and Debela, T., "Implementation of optimal load balancing strategy for hybrid energy management system in DC/AC microgrid with PV and battery storage," *International Journal of Engineering, Transactions A: Basics*, Vol. 32, (2019), 1437-1445. DOI: 10.5829/IJE.2019.32.10A.13.
- Gholami, M., "Islanding detection method of distributed generation based on wavenet," *International Journal of Engineering, Transactions B: Applications*, Vol. 32, (2019), 242-248. DOI: 10.5829/IJE.2019.32.02b.09.
- Heidari, M., and Tarafdar Hagh, M., "Optimal reconfiguration of solar photovoltaic arrays using a fast parallelized particle swarm optimization in confront of partial shading," *International Journal of Engineering, Transactions B: Applications*, Vol. 32, (2019), 1177-1185. DOI: 10.5829/IJE.2019.32.08B.14.
- Han, H., Hou, X., Yang, J., Wu, J., Su, M., and Guerrero, J. M., "Review of power sharing control strategies for islanding operation of AC microgrids," *IEEE Transactions on Smart Grid*, Vol. 7, (2016), 200-215. DOI: 10.1109/TSG.2015.2434849.
- He, J., Pan, Y., Liang, B., and Wang, C., "A simple decentralized islanding microgrid power sharing method without using droop control," *IEEE Transactions on Smart Grid*, Vol. 9, (2018), 6128-6139. DOI: 10.1109/TSG.2017.2703978.
- Chauhan, R. K., and Chauhan, K., "Distributed energy resources in Microgrid: integration, challenges and optimization," *Elsevier*, (2019), 33-56, (Chapter 2). DOI: 10.1016/B978-0-12-817774-7.00002-8.
- Mondal, A., Illindala, M. S., Khalsa, A. S., Klapp, D. A., and Eto, J. H., "Design and operation of smart loads to prevent stalling in a microgrid," *IEEE Transactions on Industry Applications*, Vol. 52, (2016), 1184-1192. DOI: 10.1109/TIA.2015.2483579.
- Lashkar Ara, A., Bagheri Tolabi, H., and Hosseini, R., "Dynamic modeling and controller design of distribution static compensator in a microgrid based on combination of fuzzy set and galaxy-based search algorithm," *International Journal of Engineering-Transactions A: Basics*, Vol. 29, (2016), 1392-1400. DOI: 10.5829/idosi.ije.2016.29.10a.10.
- Lu, X., Yu, X., Lai, J., Wang, Y., and Guerrero, J. M., "A novel distributed secondary coordination control approach for islanded microgrids," *IEEE Transactions on Smart Grid*, Vol. 9, (2018), 2726-2740. DOI: 10.1109/TSG.2016.2618120.
- Nutkani, I. U., Loh, P. C., Wang, P., and Blaabjerg, F., "Linear decentralized power sharing schemes for economic operation of AC microgrids," *IEEE Transactions on Industrial Electronics*, Vol. 63, (2016), 225-234. DOI: 10.1109/TIE.2015.2472361.
- Mahmood, H., Michaelson, D., and Jiang, J., "Accurate reactive power sharing in an islanded microgrid using adaptive virtual impedances," *IEEE Transactions on Power Electronics*, Vol. 30, (2015), 1605-1617. DOI: 10.1109/TPEL.2014.2314721.
- Lou, G., Gu, W., Xu, Y., Cheng, M., and Liu, W., "Distributed MPC-based secondary voltage control scheme for autonomous droop-controlled microgrids," *IEEE Transactions on Sustainable Energy*, Vol. 8, (2017), 792-804. DOI: 10.1109/TSTE.2016.2620283.
- Lai, J., Zhou, H., Lu, X., Yu, X., and Hu, W., "Droop-based distributed cooperative control for microgrids with time-varying delays," *IEEE Transactions on Smart Grid*, Vol. 7, (2016), 1775-1789. DOI: 10.1109/TSG.2016.2557813.
- Wu, X., and Shen, C., "Distributed optimal control for stability enhancement of microgrids with multiple distributed generators," *IEEE Transaction on Power Systems*, Vol. 32, (2017), 4045-4059. DOI: 10.1109/TPWRS.2017.2651412.
- Yu, K., Ai, Q., Wang, S., Ni, J., and Lv, T., "Analysis and optimization of droop controller for microgrid system based on small-signal dynamic model," *IEEE Transactions on Smart Grid*, Vol. 7, (2016), 695-705. DOI: 10.1109/TSG.2015.2501316.
- Kim, J., Guerrero, J. M., Rodriguez, P., Teodorescu, R., and Nam, K., "Mode adaptive droop control with virtual output impedances for an inverter-based flexible AC microgrid," *IEEE Transactions Power Electronics*, Vol. 26, (2011), 689-701. DOI: 10.1109/TPEL.2010.2091685.
- Zhang, J., Shu, J., Ning, J., Huang, L., and Wang, H., "Enhanced proportional power sharing strategy based on adaptive virtual impedance in low-voltage networked microgrid," *IET Generation, Transmission & Distribution*, Vol. 12, (2018), 2566-2576. DOI: 10.1049/iet-gtd.2018.0051.
- Zhong, Q. -C., "Robust droop controller for accurate proportional load sharing among inverters operated in parallel," *IEEE Transactions on Industrial Electronics*, Vol. 60, (2013), 1281-1290. DOI: 10.1109/TIE.2011.2146221.

22. Zhang. M., Song. B., and Wang. J., "Circulating current control strategy based on equivalent feeder for parallel inverters in islanded microgrid," *IEEE Transactions on Power Systems*, Vol. 34, (2019), 595-605. DOI: 10.1109/TPWRS.2018.2867588.
23. Chen. J., Yue. D., Dou. C., Chen. L., Weng. S., and Li. Y., "A virtual complex impedance based  $P-\dot{V}$  droop method for parallel-connected inverters in low-voltage AC microgrids," *IEEE Transactions on Industrial Informatics*, Vol. 17, (2021), 1763-1773. DOI: 10.1109/TII.2020.2997054.
24. Lee. C. -T, C. Chu. -C, and Cheng. P. -T., "A new droop control method for the autonomous operation of distributed energy resource interface converters," *IEEE Transactions on Power Electronics*, Vol. 28, (2013), 1980-1993. DOI: 10.1109/TPEL.2012.2205944.
25. Zhou, J., and Cheng, P. "A modified  $Q-\dot{V}$  droop control for accurate reactive power sharing in distributed generation microgrid," *IEEE Transactions on Industry Applications*, Vol. 55, (2019), 4100-4109. DOI: 10.1109/TIA.2019.2903093.
26. Hu. J., Zhu. J., Dorrell. D. G., and Guerrero. J. M., "Virtual flux droop method—A new control strategy of inverters in microgrids," *IEEE Transactions on Power Electronics*, Vol. 29, (2014), 4704-4711. DOI: 10.1109/TPEL.2013.2286159.
27. Ashabani. M., Mohamed. Y. A. -R. I., Mirsalim. M., and Aghashabani. M., "Multivariable droop control of synchronous current converters in weak grids/microgrids with decoupled dq-axes currents," *IEEE Transactions on Smart Grid*, Vol. 6, (2015), 1610-1620. DOI: 10.1109/TSG.2015.2392373.
28. Heydari. R., Dragicevic. T., and Blaabjerg. F., "High-bandwidth secondary voltage and frequency control of VSC-based AC microgrid," *IEEE Transactions on Power Electronics*, Vol. 34, (2019), 11320-11331. DOI: 10.1109/TPEL.2019.2896955.
29. Gdaim. S., Mtibaa. A., and Mimouni. M. F., "Design and experimental implementation of DTC of an induction machine based on fuzzy logic control on FPGA," *IEEE Transactions Fuzzy Systems*, Vol. 3, (2015), 644-655. DOI: 10.1109/TFUZZ.2014.2321612.
30. Uddin. M. N., and Hafeez. M., "FLC-based DTC scheme to improve the dynamic performance of an IM drive," *IEEE Transactions on Industry Applications*, Vol. 48, (2012), 823-831. DOI: 10.1109/TIA.2011.2181287.
31. Solat. A. R., Ranjbari. A. M., and Mozafari. B., "Coordinated control of doubly fed induction generator virtual inertia and power system oscillation damping using fuzzy logic," *International Journal of Engineering, Transactions A: Basics*, Vol. 32, (2019), 536-547. DOI: 10.5829/IJE.2019.32.04A.11.
32. El Ouanjli. N., Motahhir. S., Derouich. A., El Ghzizal. A., Chebabhi. A., and Taoussi. M., "Improved DTC strategy of doubly fed induction motor using fuzzy logic controller," *Energy Reports*, Vol. 5, (2019), 271-279. DOI: 10.1016/j.egy.2019.02.001.

---

### Persian Abstract

---

#### چکیده

در این مقاله یک استراتژی کنترل جدید برای ریزشبه جزیره‌ای مبتنی بر کنترل مشخصه افی شار مجازی (VFD) پیشنهاد شده است. در روش مرسوم مشخصه افی شار مجازی از تکنیک کنترل مستقیم شار (DFC) برای تولید سیگنال‌های کلیدزنی استفاده می‌شود که مبتنی بر تنظیم‌کننده‌های هیستریزس و جدول کلیدزنی است. بنابراین، ایجاد موجک ولتاژ و جریان اجتناب‌ناپذیر است. علاوه بر این، در هر دوره تناوب کنترلی، تنها یک بردار کلیدزنی اعمال می‌شود و از آنجایی که هیچ یک از بردارهای کلیدزنی نمی‌توانند ولتاژ مورد نظر را تولید کنند، عملکرد دینامیکی مطلوب حاصل نمی‌شود. در اینجا، روش جدید کنترل فازی شار مستقیم (DFFC) برای انتخاب بهترین بردار کلیدزنی بر اساس منطق فازی پیشنهاد شده است. همچنین، فقط کسری از دوره تناوب کنترل به یک بردار کلیدزنی فعال مناسب اختصاص داده می‌شود که با روش کنترل فازی شار مستقیم انتخاب می‌شود؛ در حالی که زمان باقی‌مانده از دوره تناوب کنترل به یک بردار کلیدزنی صفر اختصاص می‌یابد. زمان وظیفه بردار کلیدزنی فعالی که انتخاب شده است با استفاده از مکانیسمی ساده و مقاوم به طور بهینه تعیین می‌شود. به منظور ارزیابی عملکرد روش پیشنهادی، یک ریز شبکه جزیره‌ای و استراتژی کنترل پیشنهادی در نرم افزار Matlab/Simulink شبیه‌سازی شده است. نتایج ثابت می‌کند که پاسخ عملکرد دینامیکی بهبود می‌یابد و توان مورد نیاز بار به طور متناسب بین منابع تولید توان، تقسیم می‌شود، در حالی که موجک ولتاژ و جریان به طور چشمگیری کاهش می‌یابد.

---